Practical Implementation and Operational Experience of Dynamic Mode Decomposition in Wide-area Monitoring Systems of Italian Power System

Andrea Vicario, Alberto Berizzi, Giorgio Maria Giannuzzi, and Cosimo Pisani

***Abstract*—This study presents the assumptions and strategies for the practical implementation of the dynamic mode decomposition approach in the wide-area monitoring system of the Italian transmission system operator, Terna. The procedure set up aims to detect poorly damped power system interarea oscillations. Dynamic mode decomposition is a data-driven technique that has gained increasing attention in different fields; the proposed implementation can both characterize the oscillatory modes and identify the most influenced areas. This study presents the results of its real-life implementation and operational experience in power system monitoring. It focuses on the main characteristics and solutions identified to reliably monitor the interarea electromechanical modes of the interconnected European power system. Moreover, conditions to issue an appropriate alarm in case of critical operating conditions are described. The effectiveness of the proposed approach is validated by its application in three case studies: a critical oscillatory event and a short-circuit event that occurred in the Italian power system in the previous years, and a 15-minute time interval of normal grid operation recorded in March 2021.**

***Index Terms*—Power system control, power system dynamics, wide-are monitoring system (WAMS), dynamic mode decomposition.**

I. Introduction

THE growth of non-programmable renewable energy sources (RES) (likely to accelerate in the next few years owing to the de-carbonizing policies adopted in Europe and worldwide) has enabled transmission system operators (TSOs) to identify the most suitable functions to guarantee the security of power systems. Accordingly, the significant deployment of phasor measurement units (PMUs) for wide-area monitoring systems (WAMSs) may be of paramount importance, provided suitable methods and algorithms to elaborate the massive stream of data are available to both extract significant information in real-time and provide alarms in the case of critical operating conditions.

Presently, interarea oscillations are critical because they are likely to move a large amount of power across interconnections unless they are immediately damped. Consequently, these oscillations can trigger cascading events, potentially leading to large blackouts.

Moreover, the occurrence of poorly damped interarea oscillations is increasing (for example, in the European power system [1], [2]). Hence, to preserve system stability, it is necessary to ① promptly identify them in both perturbed and normal operating conditions, ② characterize them in real-time, and ③ determine and establish suitable countermeasures.

The characterization of the electromechanical modes aims to estimate their magnitude, frequency, and damping. Many algorithms are available in the technical literature to simultaneously perform these three goals, starting from PMU data with different properties in terms of accuracy and robustness. For instance, they can be based on the Hilbert transform [3]-[5], which enables the estimation of the damping of the oscillatory modes with high accuracy, particle swarm optimization [6], characterized by a good accuracy of the estimated parameters, or the wavelet-based method [7], which decomposes signals into functions of both time and frequency domains. However, a complete characterization of the oscillatory modes, identifying the areas involved and the phase displacement of oscillations (mode shapes) cannot be performed using the aforementioned methodologies. Other methods have also been investigated, for example, those based on principal component analysis [8], which can provide a robust and accurate evaluation of magnitude, frequency, and damping of oscillatory modes, giving at the same time information on the areas more affected by each mode. However, this methodology cannot completely characterize the mode shapes associated in terms of phase displacement.

Dynamic mode decomposition (DMD) has recently gained the interest of power system researchers, both for post-disturbance and ambient data analysis, owing to its accuracy, robustness, and information content, resulting from optimiza-

Manuscript received: July 28, 2021; revised: January 19, 2022; accepted: June 24, 2022. Date of CrossCheck: June 24, 2022. Date of online publication: XX XX, XXXX.

A. Vicario (corresponding author) and A. Berizzi are with the Department of Energy at Politecnico di Milano, Milan, Italy (e-mail: andrea.vicario@polimi.it; alberto.berizzi@polimi.it).

G. M. Giannuzzi and C. Pisani are with Terna S.p.A., Rome, Italy (e-mail: giorgio.giannuzzi@terna.it; cosimo.pisani@terna.it).

DOI: 10.35833/MPCE.2021.000509

tion over a time window. In addition, the computational complexity of DMD is limited, which enables the real-time exploitation of its properties. DMD provides modal decomposition, where each mode comprises spatially correlated structures that have the same linear behavior over time. First applied to fluid dynamics in [9] and deeply studied in [10], DMD has been proposed in many alternative algorithms, mainly developed to overcome some of its intrinsic weaknesses, particularly in the case of noisy datasets.

References [11] and [12] proposed the first version of the DMD to monitor electromechanical modes; the "exact DMD formulation", presented in [10], has been adopted for modal estimation of power systems in [13]. Optimized DMD [14] or robust DMD, based on robust principal component analysis [15], are alternative methods of avoiding corruption and noise in datasets. Block-enhanced DMD [16], which is based on the Hankel matrix, improves the ability to capture mode information from ambient data. This approach (also called data stacking) was proposed in [17] and combined with an optimal hard threshold to select the best model order to deal with noise. Nonlinear observables [18] can extend the DMD to better capture the system dynamics. Randomized DMD combined with data stacking [19] can increase the computing efficiency without losing accuracy. In [20], the output-only observer/Kalman filter identification was used to process the ambient data, followed by the DMD to characterize the frequency and damping.

Finally, DMD was applied to identify synchronous machine coherency in post-fault conditions [21]. In [22], the rotor angle and acceleration of synchronous machines during a fault were predicted using DMD. In [22], extended-DMD was used for dynamic state estimation in real time, whereas DMD was used for inertia estimation in [23]. In [24], the output results of the DMD were used as a reference to validate a machine learning approach.

Based on a review of the technical literature, research on DMD theory has developed and has been applied to both synthetic and real data (e. g., [11], [13], [16], [18], [19] based on the analysis of real ring-down events and ambient data). Particularly, DMD proved its effectiveness in the analysis of data recorded during oscillatory events.

However, its ability during fast transient such as short circuits or normal load variation and the possibility of issuing alarms in case of critical operating conditions is yet to be reported. Moreover, real-life DMD implementation in a TSO control room is still undocumented. This study aims to fill this gap by providing the operational experience of using DMD in a TSO control center where the data stream from WAMS is processed. The DMD output was used to monitor and control the Italian power system in its interconnected operation with the European power system.

The main contributions of this study are as follows:

1) Application of DMD to detect and characterize oscillatory interarea modes (frequency, amplitude, damping, and mode shapes), which must be reliable and robust under both transient (under different types of perturbations) and normal operating conditions.

2) Determination of conditions to issue alarms for the control room to trigger possible countermeasures.

3) Analysis of DMD properties in the presence of ambient signals characterized by factors such as noise, changes of operating conditions, and topology.

The aforementioned contributions were identified after a one-year test campaign conducted on the Italian power system. The results presented in this study show very good robustness under all different power system conditions and very good accuracy compared with other DMD approaches tested. In addition, the identification of mode shapes was accurate and in agreement with the operational experience of control room engineers and ENTSO-E studies.

The remainder of this paper is organized as follows: the DMD theory is presented in Section II, whereas Section III focuses on its practical implementation in Terna control center, with the underlying criteria to issue alarms and trigger control actions. Section IV presents some selected results focusing on the operating conditions and perturbations that can be critical to accurately identifying modal power system properties. Two events occurred in the Italian power system in the last few years, and a 15-minute time interval of normal grid operation recorded in March 2021 were analyzed. The results show very good robustness and accuracy of the adopted technique and implementation.

II. DMD Theory

This section presents the theory of the DMD implemented for the security monitoring module and the identification of the dominant modes and their features. The DMD utilizes singular value decomposition (SVD) to obtain dimensionality reduction in high-dimensional systems [25]. The DMD adopted uses the exact DMD [10], [13] combined with the block-enhanced formulation, as proposed by [16], [17] for power systems.

A. Exact DMD Architecture

This subsection briefly discusses the theory of exact DMD [10], [13]. Data are collected from a generic nonlinear system with unknown dynamics. The data from the measurements are used to approximate the dynamics with locally linear systems:

$$\frac{\mathrm{d}\boldsymbol{x}}{\mathrm{d}t}=\boldsymbol{A}\boldsymbol{x} \tag{1}$$

where $\boldsymbol{x}$ is a vector representing the states of the dynamic system at a generic time t; and $\boldsymbol{A}$ is the constant matrix describing the dynamic system. Discretizing (1) with sampling time Δt, we can obtain:

$$\boldsymbol{x}_{k+1}=\boldsymbol{B}\boldsymbol{x}_k \tag{2}$$

$$\boldsymbol{B}=\mathrm{e}^{\boldsymbol{A}\Delta t} \tag{3}$$

Matrices $\boldsymbol{A}$ and $\boldsymbol{B}$ have the same eigenvectors $\boldsymbol{\phi}_j$ and their eigenvalues are such that $\lambda_k=\mathrm{e}^{\omega_k\Delta t}$, where λ_k is the k^{th} eigenvalue of $\boldsymbol{B}$ and ω_k is the k^{th} eigenvalue of $\boldsymbol{A}$.

The DMD performs a low-rank projection of $\boldsymbol{B}$, indicated by $\tilde{\boldsymbol{B}}$, which optimally fits the measured data by minimizing the error ε:

$$\varepsilon=\left\|\boldsymbol{x}_{k+1}-\tilde{\boldsymbol{B}}\boldsymbol{x}_k\right\|_2 \tag{4}$$

This approximation holds only over the sampling window where $\tilde{\boldsymbol{B}}$ is built. To compute $\tilde{\boldsymbol{B}}$ and minimize ε across all snapshots $k=1,2,\ldots,m$, the n measurements for each of the m snapshots can be arranged into two data matrices $\boldsymbol{X}$ and $\boldsymbol{X}'$ and the exact DMD can be carried out. The measurements are stored in a matrix $\boldsymbol{X}$ organized as follows: data related to the same snapshot are stored in the same column and data from the same PMU are stored in the same row. $\boldsymbol{X}'$ has the same structure; however, data are time-shifted by Δt.

$$\boldsymbol{X}=\overbrace{\begin{bmatrix} | & | & \cdots & | \\ \boldsymbol{x}_1 & \boldsymbol{x}_2 & \cdots & \boldsymbol{x}_{m-1} \\ | & | & \cdots & | \end{bmatrix}}^{m-1 \text{ snapshots}} \tag{5}$$

$$\boldsymbol{X}'=\begin{bmatrix} | & | & \cdots & | \\ \boldsymbol{x}_2 & \boldsymbol{x}_3 & \cdots & \boldsymbol{x}_m \\ | & | & \cdots & | \end{bmatrix}\Bigg\downarrow n \text{ PMUs} \tag{6}$$

Thus, (2) can be rewritten as:

$$\boldsymbol{X}'=\boldsymbol{B}\boldsymbol{X} \tag{7}$$

Hence, matrix $\boldsymbol{B}$ is written as:

$$\boldsymbol{B}=\boldsymbol{X}'\boldsymbol{X}^{\dagger} \tag{8}$$

where † represents the Moore-Penrose pseudoinverse [26]. Thus, rank truncation can be performed to consider only a limited number r of dominant modes; the exact DMD approach computes a rank-reduced representation in terms of a proper orthogonal decomposition (POD) projected matrix $\tilde{\boldsymbol{B}}$. Hence, the data matrix can be approximated using its SVD:

$$\boldsymbol{X}\approx\boldsymbol{U}_{\mathrm{r}}\boldsymbol{\Sigma}_{\mathrm{r}}\boldsymbol{V}_{\mathrm{r}}^{*} \tag{9}$$

where $\boldsymbol{U}_{\mathrm{r}}$, $\boldsymbol{\Sigma}_{\mathrm{r}}$, and $\boldsymbol{V}_{\mathrm{r}}$ have the dimensions of $n\times r$, $r\times r$, and $(m-1)\times r$, respectively; and * denotes the conjugate transpose. Thus, $\boldsymbol{B}$ can be efficiently projected onto the POD modes, and the upper triangular matrix $\tilde{\boldsymbol{B}}$ is obtained as:

$$\tilde{\boldsymbol{B}}=\boldsymbol{U}_{\mathrm{r}}^{*}(\boldsymbol{X}'\boldsymbol{V}_{\mathrm{r}}\boldsymbol{\Sigma}_{\mathrm{r}}^{-1}\boldsymbol{U}_{\mathrm{r}}^{*})\boldsymbol{U}_{\mathrm{r}}=\boldsymbol{U}_{\mathrm{r}}^{*}\boldsymbol{X}'\boldsymbol{V}_{\mathrm{r}}\boldsymbol{\Sigma}_{\mathrm{r}}^{-1} \tag{10}$$

$\tilde{\boldsymbol{B}}$ defines the low-dimensional linear model of a dynamic system. To identify the mode properties, frequencies, damping, and mode shapes, the eigenvalue problem for $\tilde{\boldsymbol{B}}$ is solved as:

$$\tilde{\boldsymbol{B}}\boldsymbol{W}_{\mathrm{r}}=\boldsymbol{W}_{\mathrm{r}}\boldsymbol{\Lambda}_{\mathrm{r}} \tag{11}$$

where the columns of matrix $\boldsymbol{W}_{\mathrm{r}}$ $(r\times r)$ are the eigenvectors; and $\boldsymbol{\Lambda}_{\mathrm{r}}$ is a diagonal matrix $(r\times r)$ containing the eigenvalues λ_j of $\tilde{\boldsymbol{B}}$. Finally, $\boldsymbol{B}$ can be reconstructed from $\boldsymbol{W}_{\mathrm{r}}$ and $\boldsymbol{\Lambda}_{\mathrm{r}}$; a subset of the eigenvalues of $\boldsymbol{B}$ is provided by $\boldsymbol{\Lambda}_{\mathrm{r}}$, whereas a subset of its eigenvectors $\boldsymbol{\phi}_j$ is provided by the columns of $\boldsymbol{\Phi}_{\mathrm{r}}$ $(n\times r)$ (the "exact DMD modes"):

$$\boldsymbol{\Phi}_{\mathrm{r}}=\boldsymbol{X}'\boldsymbol{V}_{\mathrm{r}}\boldsymbol{\Sigma}_{\mathrm{r}}^{-1}\boldsymbol{W}_{\mathrm{r}} \tag{12}$$

Finally, the approximated solution for all future time is:

$$\boldsymbol{x}(t)\approx\sum_{j=1}^{r}\boldsymbol{\phi}_j\exp(\omega_j t)b_{rj}=\boldsymbol{\Phi}_{\mathrm{r}}\exp(\boldsymbol{\Omega}_{\mathrm{r}}t)\boldsymbol{b}_{\mathrm{r}} \tag{13}$$

where $\omega_j=\ln(\lambda_j)/\Delta t$ is the j^{th} eigenvalue of $\boldsymbol{A}$ in the continuous-time domain; $\boldsymbol{b}_{\mathrm{r}}$ is a vector, whose elements b_{rj} are the initial amplitudes of each DMD mode. This can be computed from the first snapshot $\boldsymbol{x}_1$ at $t=0$ in (13).

$$\boldsymbol{x}_1\approx\boldsymbol{\Phi}_{\mathrm{r}}\boldsymbol{b}_{\mathrm{r}} \tag{14}$$

Because $\boldsymbol{\Phi}_{\mathrm{r}}$ is generally a non-square matrix, $\boldsymbol{b}_{\mathrm{r}}$ is computed by finding the best-fit solution using the least-squares method:

$$\boldsymbol{b}_{\mathrm{r}}=\boldsymbol{\Phi}_{\mathrm{r}}^{\dagger}\boldsymbol{x}_1 \tag{15}$$

The frequency f and damping ratio ξ of the identified modes are computed from the continuous-time eigenvalues $(\omega_j=\alpha\pm\mathrm{i}\beta)$:

$$f=\frac{\beta}{2\pi} \tag{16}$$

$$\xi=\frac{-\alpha}{\sqrt{\alpha^2+\beta^2}} \tag{17}$$

Finally, the mode shapes of the processed measurements are obtained from the columns of $\boldsymbol{\Phi}_{\mathrm{r}}$ in (12).

B. Block-enhanced Formulation Considering Time-delay Coordinates for DMD

This study adopts a block-enhanced formulation using an augmented set of coordinates built by considering the time-delay coordinates. Time-delay coordinates [25] are used to reconstruct the dynamics of systems that do not have sufficient measurements, even allowing the estimation of modal parameters from a single PMU. They can be obtained by stacking s times the vector of measurements $\boldsymbol{x}$, building the $((n\times s)\times(m-s+1))$ Hankel matrix $\boldsymbol{H}$:

$$\boldsymbol{H}=\begin{bmatrix} \begin{bmatrix} | \\ \boldsymbol{x}_1 \\ | \end{bmatrix} & \begin{bmatrix} | \\ \boldsymbol{x}_2 \\ | \end{bmatrix} & & \begin{bmatrix} | \\ \boldsymbol{x}_{m-s+1} \\ | \end{bmatrix} \\ \begin{bmatrix} | \\ \boldsymbol{x}_2 \\ | \end{bmatrix} & \begin{bmatrix} | \\ \boldsymbol{x}_3 \\ | \end{bmatrix} & \cdots & \begin{bmatrix} | \\ \boldsymbol{x}_{m-s+2} \\ | \end{bmatrix} \\ \vdots & \vdots & & \vdots \\ \begin{bmatrix} | \\ \boldsymbol{x}_s \\ | \end{bmatrix} & \begin{bmatrix} | \\ \cdots \\ | \end{bmatrix} & & \begin{bmatrix} | \\ \boldsymbol{x}_m \\ | \end{bmatrix} \end{bmatrix} \tag{18}$$

Thus, the block-enhanced formulation involves applying the exact DMD to matrices $\boldsymbol{X}$ and $\boldsymbol{X}'$ derived from $\boldsymbol{H}$:

$$\boldsymbol{X}=\begin{bmatrix} | & | & \cdots & | \\ \boldsymbol{H}_1 & \boldsymbol{H}_2 & \cdots & \boldsymbol{H}_{m-s} \\ | & | & \cdots & | \end{bmatrix} \tag{19}$$

$$\boldsymbol{X}'=\begin{bmatrix} | & | & \cdots & | \\ \boldsymbol{H}_2 & \boldsymbol{H}_3 & \cdots & \boldsymbol{H}_{m-s+1} \\ | & | & \cdots & | \end{bmatrix} \tag{20}$$

If the measurement set is low-dimensional, the rank of $\boldsymbol{H}$ may be increased using more time-delay coordinates. The number of time-delay coordinates s may be increased until the system reaches full rank [10].

C. Mode Ranking

The DMD can extract the most important spatio-temporal patterns and eigenvalues from a dataset; however, the mode ranking resulting from the DMD is not necessarily in agreement with the energy content. Therefore, a criterion should

be determined to select the dominant modes (accordingly, [27], [28] first identify dominant modes from data-driven estimation methods). In [10], the initial mode amplitude evaluation is proposed according to (15); however, this solution only considers the initial conditions and not the mode evolution over time. Different solutions can be found in previous studies to associate each mode with a pseudo-energy. For example, in [11], the ranking is based on a combination of the right eigenvectors, the right singular vector, and its singular values. The method based on [29] is instead adopted in [13] to rank the modes and identify the dominant modes. For each mode j, the associated energy E_j is computed as:

$$E_j = \left| b_{rj} \mathrm{e}^{\omega_j T} \right| \tag{21}$$

where T is the time window considered. Here, the ranking is not based on the behavior of a single point in time but takes into account the whole time window; modes are finally ranked according to their energy and those presenting the largest values are assumed to be dominant. As confirmed by simulations and tests, the DMD can generate spurious modes with damping and frequency similar to actual modes [13] for different system orders and different sizes of the time window considered. This is the only drawback observed during all the tests performed on the DMD implemented.

Finally, another criterion to identify dominant modes in real-time is based on [30], which utilizes the Riccati equation, searching for the optimal mode amplitude b_{rj} that minimizes the l_2 error between $\boldsymbol{X}$ and the approximation in (22) (more details are provided in [30]).

$$\boldsymbol{X} \approx \begin{bmatrix} | & | & | \\ \phi_{r1} & \phi_{r2} & \cdots \\ | & | & | \end{bmatrix} \begin{bmatrix} b_{r1} & 0 & \cdots & 0 \\ 0 & b_{r2} & \cdots & 0 \\ \vdots & \vdots & \cdots & \vdots \\ 0 & 0 & \cdots & b_{rj} \end{bmatrix} \begin{bmatrix} 1 & \lambda_{r1} & \cdots & \lambda_{r1}^{m-1} \\ 1 & \lambda_{r2} & \cdots & \lambda_{r2}^{m-1} \\ \vdots & \vdots & \cdots & \vdots \\ 1 & \lambda_{rj} & \cdots & \lambda_{rj}^{m-1} \end{bmatrix} \tag{22}$$

The computed optimal b_{rj} is then associated with each identified mode. This index is selected for the final implementation because the tests reported in Section IV indicate that the first two approaches may result in false alarms.

III. Practical Implementation of DMD Approach

This section describes the practical implementation of the DMD approach in Terna control center. The practical choice of the most suitable type of DMD, filtering of input data, selection of the most suitable index to issue alarms, and information visualization to control room operators are described.

As the DMD approach implemented is tailored for the Italian power system within continental Europe, the main interest of the Italian TSO is to detect the interarea modes involving the Italian power system. The modes with the highest participation factors of Italian power plants are the principal focus, especially those characterized by a frequency ranging from 0.24 to 0.35 Hz, as involved in real events [2] and previous studies [13]. This mode, also known as the South-North (S-N) European mode, shows that the Italian power system is in phase opposition to the rest of the northern European power system. Because the largest oscillatory events are better observable in southern Italy ([2], [13]), most of the processed PMUs are placed in this portion of the system.

The DMD implemented in Terna control center uses the exact DMD with the block-enhanced formulation and elaborates the data stream (sampled at 50 Hz, i.e., a sample every 20 ms) from the n PMUs available from the WAMS system (generally, 20 PMUs are processed). The input data stream is a 20 s sliding window; this time-window length has been selected as a good compromise between the stability of the results over time and the quick response of the monitoring tool. It can be changed by the user if necessary.

Data streams from the field are properly processed to address issues such as noise or missing elements that could influence the real data flow: ① data detrending; ② data packet reconstruction, i. e., fill missing values; ③ data filtering via a Hilbert bandpass filter to maintain only typical frequencies of the main European interarea modes (0.10-0.50 Hz), discarding slower (control) modes and faster modes (local) [31]).

All available voltage, frequencies, magnitudes, angles, and real and reactive power flows (measured by PMUs) can be used as inputs to the DMD. However, rank truncation typically detects and discards redundant information. Busbar frequencies alone can be used for this application and provide good observability of the interarea mode (thus saving computation time, according to the real-time requirements of the tool). Moreover, as power systems generally present a low-rank pattern [13], based on experience, a rank truncation to the first eight singular values is sufficiently accurate to observe the main interarea modes of the interconnected European power system.

The knowledge of mode shape is among the key factors and very good property of DMD compared with other approaches, as it enables the understanding of the coherency properties of the system. This knowledge is important, particularly in the case of re-dispatching actions, power reduction, or even disconnection of the generator(s). Generators with the highest participation factor have the highest damping effect on ongoing oscillation. The main goal of the proposed application is to issue an alarm for control room operators in the case of critical interarea oscillations. Hence, the observed modes should be ranked and a suitable index should be selected to be compared with a threshold to generate an alarm or apply an automatic control action. The monitoring of individual mode amplitudes and the relevant damping alone might lead to false alarms; adopting as indices, the initial amplitude from (15) shows unsatisfactory performance, whereas the choice of (21) shows unstable behavior, as demonstrated in Section IV.

Based on the aforementioned findings, the monitoring system triggers an alarm if all the following three conditions are fulfilled for each 20 s window processed:

1) The DMD detects the presence of at least one mode with a frequency within the aforementioned range (0.24-0.35 Hz). Notably, the control room displays continuously show modal frequency, amplitude, and associated mode shapes.

2) The optimal amplitude b_m for the 0.24/0.35 Hz mode computed according to (22) is higher than the threshold set according to experience. This threshold is currently set at

0.10 p.u., a compromise between the need to capture all critical events and, simultaneously avoiding false alarms. Many tests have been conducted on real power systems to fix this threshold. It has been selected after long-term validation, considering the different operating conditions of the Italian power system (low/high demand), different grid topologies, generation patterns (traditional vs. renewable), and side effects such as PMU noise (estimated with a signal-to-noise ratio of 45 dB according to [32]), number of PMU processed, packet losses, and outliers in the main data stream.

3) The peak-to-peak frequency deviation is higher than 60 mHz for at least 3 cycles, proving an ongoing event.

If all these conditions are fulfilled, the alarm is set to ON, and the operator is aware that a critical interarea oscillation is in place. Manual control actions will be performed (reduction of the real power flows in critical sections or tie-lines, generator re-dispatching/disconnection, load reduction, and network topology changes, based on the system condition and operator knowledge). Automatic control actions based on wide-area power oscillation damping control activation [33], [34] (control of the active power generated) will also be implemented soon in Terna control center.

Figure 1 shows the overall flowchart of the proposed procedure.

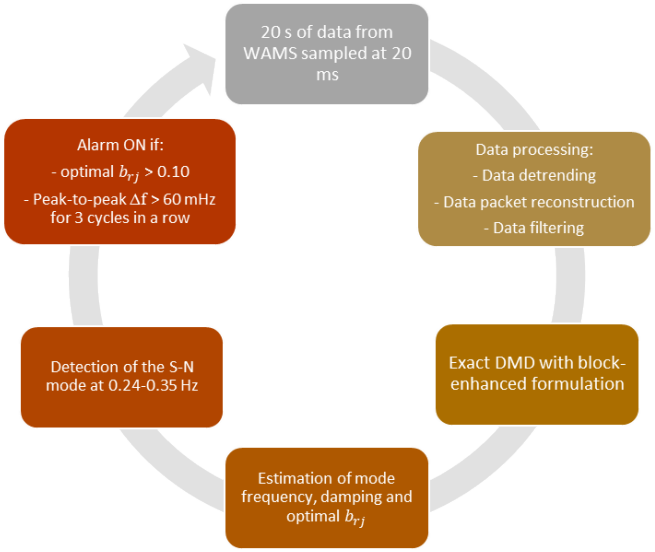

Fig. 1. Flowchart of the proposed procedure.

IV. Tests and Results

In this section, the main results obtained from the practical DMD implementation are presented and discussed, with reference to three different operating conditions, to prove both its reliability and robustness to operating conditions: a significant oscillatory event, a short-circuit event, often erroneously understood by monitoring tools as an oscillation, and a 15-minute time interval of normal grid operation. Particularly, the results of the exact DMD and block-enhanced DMD are compared with three different ranking approaches ([10], [13], [30]) in terms of detection speed.

Frequency measurements are known to be influenced by significant noise. In the preliminary tests, frequency, voltage, and power measurements are employed to feed the DMD, as heterogeneous measurements can be used for mode identification. An increasing number of signals might improve the detection of a critical oscillation if the added signals exhibit high observability for this mode. Meanwhile, highly correlated signals do not always improve identification but increase computing time [27]. Presently, the procedure is based on frequency measurements only, suitably filtered, also because the alarm is set to be ON based on a peak-to-peak frequency deviation. Moreover, not all Italian critical tie lines are currently covered by the PMU to provide real and reactive power measurements and to feed the approach.

A. Oscillatory Event of December 2017

The oscillatory event that occurred on December 3, 2017 was first extensively discussed and presented in [2] and [13] and was characterized by an undamped frequency oscillation up to approximately 300 mHz in southern Italy. It began at 01:09 and reached its maximum deviation at 01:15 Figure 2 shows the frequencies of the oscillatory event recorded at different locations of the Italian power system.

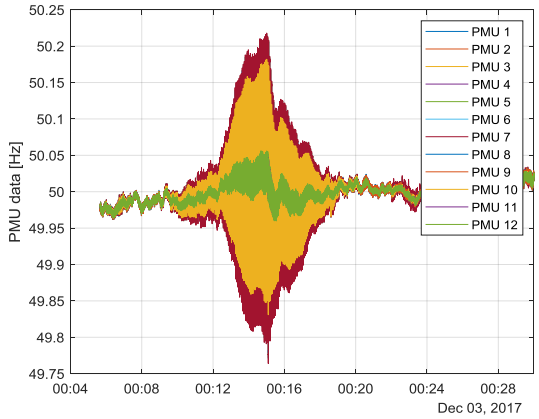

Fig. 2. Frequencies of the oscillatory event of December 3, 2017.

These oscillatory events can lead to emergencies. Therefore, the monitoring system should correctly classify the event, provide proper interpretations to operators, and suggest the most suitable corrective actions.

The frequency, damping, and amplitude of the first three modes identified by the block-enhanced DMD are shown in Fig. 3. Mode 2 presents a frequency close to 0.29-0.30 Hz and damping less than 5% all the time, as shown in Fig. 4; its amplitude, i. e., the optimal b_{rj} computed according to (22), shows an increasing pattern from 00: 10 until 00: 14. The corresponding mode shapes during the maximum frequency deviation are shown in Fig. 5. With regard to the correctness of the approach, the estimated mode shapes resulting from the DMD were compared in [13] with the traditional modal analysis results, thereby successfully validating the approach. Moreover, regarding the European power system, Fig. 5 is consistent with the studies conducted by the System Protection and Dynamics Group of ENTSO-E [2].

This event is used as a benchmark and to tune the implemented DMD; if in 2017 the DMD had been online in Terna

control center, it would have issued an alarm (the trigger signal Fig. 3) at 00:11, a few seconds after the beginning of the oscillatory event in a pronounced manner. This trigger would have been possible because all the tripping conditions described in Section III are verified. A mode with the frequency characteristics of the S-N mode is identified, the optimal b_{rj} exceeds the 0.10 threshold, and PMU frequency measurements deviate by more than 60 mHz from 50 Hz for three cycles. Hence, the DMD would have enabled prompt control by control room operators.

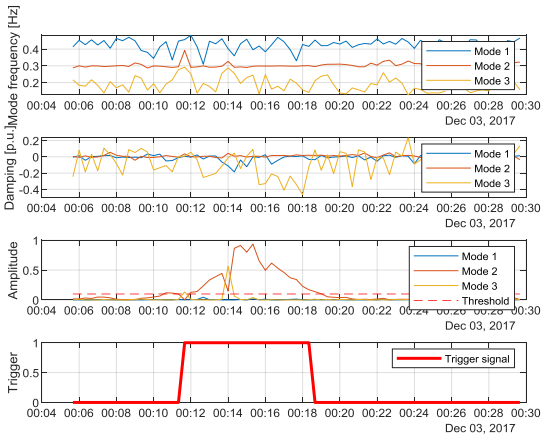

Fig. 3. Frequency, damping, and amplitude of first three modes identified by block-enhanced DMD along with trigger status.

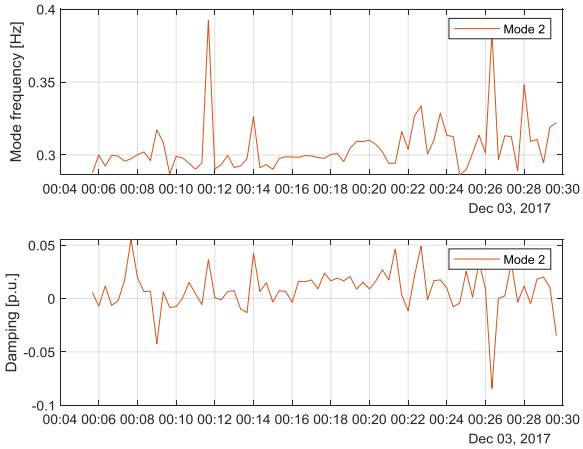

Fig. 4. Frequency and damping of Mode 2.

The other two modes identified by the block-enhanced DMD, i. e., one around 0.40-0.45 Hz (mode 1) and one around 0.20 Hz (mode 3), both show negative or zero damping values. Nevertheless, their amplitudes are not sufficient to trigger an alarm. These modes suggest the presence of unstable behavior, as their damping fluctuates significantly, even showing high negative values. However, Fig. 6 confirms that these modes are not physical because the relative frequencies do not appear in the signal spectrum; they are spurious modes caused by the DMD approximating the nonlinear system dynamics in a least-squares manner over a certain time span [13]. The proposed analysis of the optimal b_{rj} can filter these modes, and it is also useful in practical implementations. Further, damping alone cannot be used as a reliable index for grid monitoring (associated amplitude, mode shapes, and frequency must also be considered).

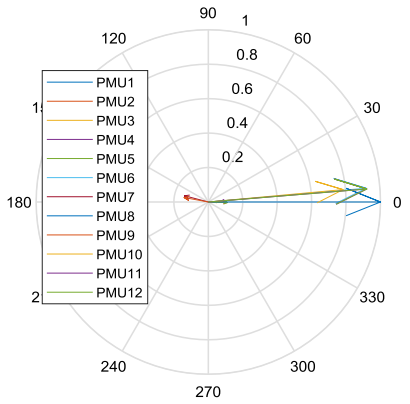

Fig. 5. Mode shapes during the maximum frequency deviation.

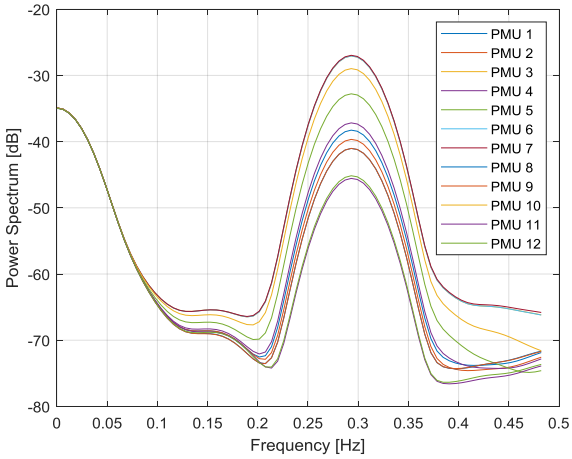

Fig. 6. Power spectrum of oscillatory event of December 3, 2017..

Other DMD-based approaches were tested on the same event shown in Fig. 2 and compared. During this assessment, attention was paid to the trigger signal to evaluate the ability of the monitoring tool to capture the alarm conditions in a timely manner.

Figure 7 shows the result of applying the exact DMD approach (not block-enhanced) using (22) as the amplitude to trigger the alarm. Two modes (1 and 2) are identified in the range of 0.24-0.35 Hz; a third mode close to 0.10 Hz sometimes appears. Furthermore, the amplitudes, i.e., the optimal b_{rj}, of modes 2 and 3 present spikes that render the identification of spurious modes possibly generated by the DMD approximation difficult. Finally, the trigger signal presents discontinuities, thus putting the operator in trouble about the decision to issue a control action.

Figure 8 shows the results obtained by the procedure applying the block-enhanced DMD adopting E_j of (21) to trigger the alarm [13]. Even if the trigger signal is correctly set to be 1 at the beginning of the oscillatory event at 00: 11, Terna discards this approach for the mode amplitude evaluation, as the threshold to be compared with E_j over time cannot be easily defined. E_j is indeed dependent on the value of

T considered and the number of processed PMUs; that is, it depends on the structure of the monitoring system (energy in Fig. 8 ranging from 0 to 10). Hence, fixing a threshold to trigger the alarm on E_j would be difficult, whereas the use of (22) has proven to be more efficient.

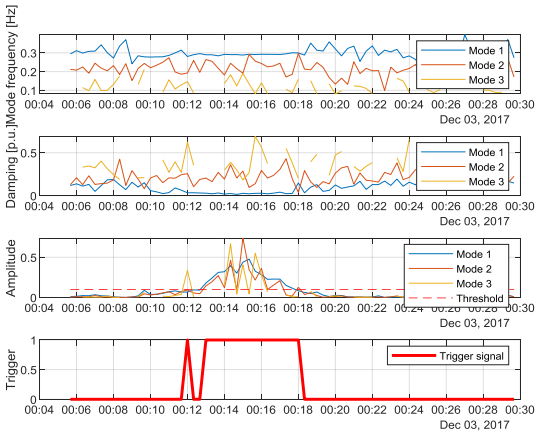

Fig. 7. Frequency, damping, and amplitude identified by exact DMD adopting *optimal* b_{rj} along with trigger status.

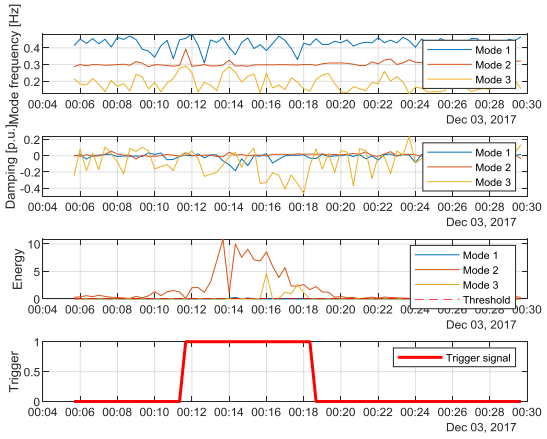

Fig. 8. Results obtained by procedure applying block-enhanced DMD adopting E_j of (21) to trigger the alarm.

Figure 9 shows the results obtained by applying the block-enhanced DMD combined with the initial amplitude (15) proposed by [10], where the trigger signal presents discontinuities, particularly at 00:13, as the mode amplitude (red line) is reduced below the threshold, which causes Terna to also discard this approach and adopt the block-enhanced DMD, together with the optimal amplitude from (22).

B. Short-circuit Event of February 2019

The second event analyzed in this study differs significantly from the first event and is a short-circuit event that occurred in the high-voltage network of the Italian power system in February 2019, as shown in Fig. 10. This event is studied to verify the selectivity of the oscillation detection, as the monitoring tool aims to issue alarms only in the case of interarea oscillation. Therefore, it is crucial to validate that the monitoring tool can distinguish interarea oscillations from other types of oscillations.

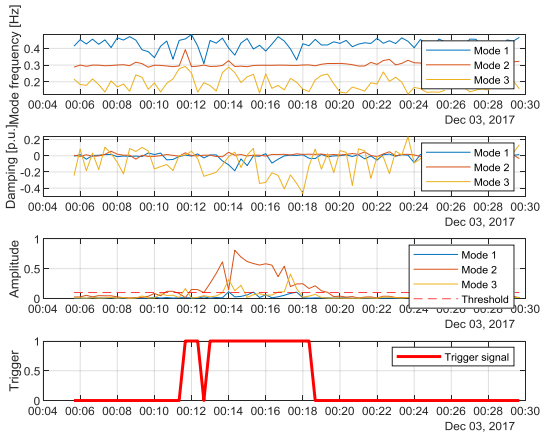

Fig. 9. Results obtained by applying block-enhanced DMD combined with initial amplitude proposed by [10].

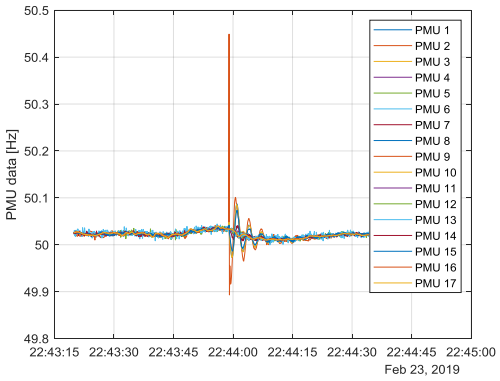

Fig. 10. Short-circuit event in February 2019.

The power spectrum of short-circuit event in February 2019 is shown in Fig. 11, where a small peak can be observed at approximately 0.25 Hz.

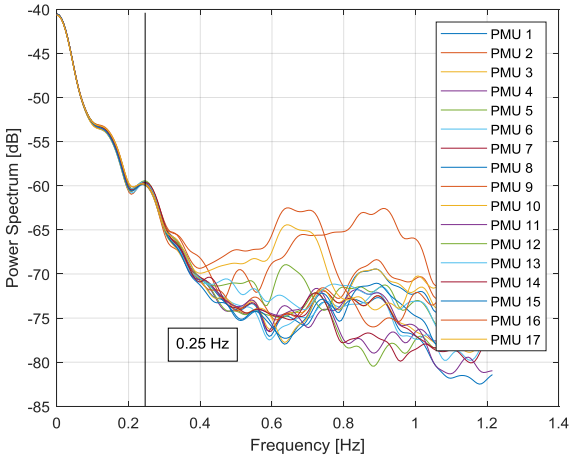

Fig. 11. Power spectrum of short-circuit event in February 2019.

The results obtained by the proposed approach are shown in Fig. 12.

The monitoring system identifies three modes ranging from 0.20 to 0.40 Hz, characterized by low or even negative damping. However, despite their negative damping, the sys-

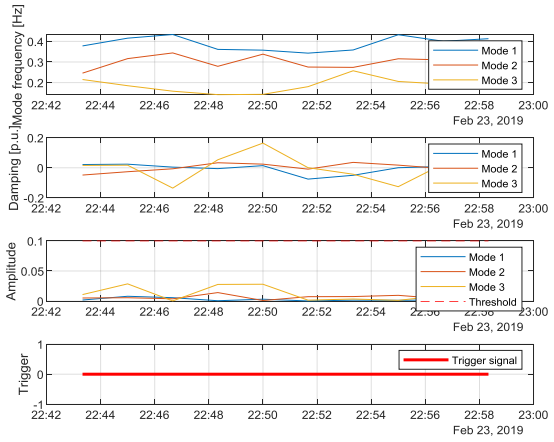

Fig. 12. Results obtained by proposed approach along with the trigger status.

tem correctly does not issue any alarm (as the S-N mode amplitude does not exceed the predefined threshold (0.1)), thus providing the correct interpretation of the phenomenon monitored.

C. Normal Grid Operation of March 2021

The third case considers all possible issues that might occur in a power system in the interval of 15 min of normal grid operation in March 2021, as shown in Fig. 13. The goal is to assess the ability of the adopted implementation to correctly identify the modes in place, although their amplitudes are not sufficiently high to make the situation critical. It can be observed that the frequency deviates around the nominal value by a maximum of 40 mHz. This deviation does not represent a critical condition; therefore, it is needless issuing an alarm to the operator. However, a poorly damped mode (purple oscillation) is present, which should be tracked by the monitoring tool. The power spectrum of the time window considered is shown in Fig. 14, which shows a peak at 0.29 Hz.

The proposed approach accurately identifies a mode at approximately 0.30 Hz (mode 2 in Fig. 15), whose energy content (measured by the value of the optimal b_{rj} from (22)) oscillates close to the threshold of 0.10. Even if its associated amplitude sometimes exceeds the defined threshold, no alarm signal is issued because the peak-to-peak frequency deviation is less than 60 mHz. Other modes are identified at approximately 0.40 and 0.20 Hz; however, their energy is very low and hence they are filtered out.

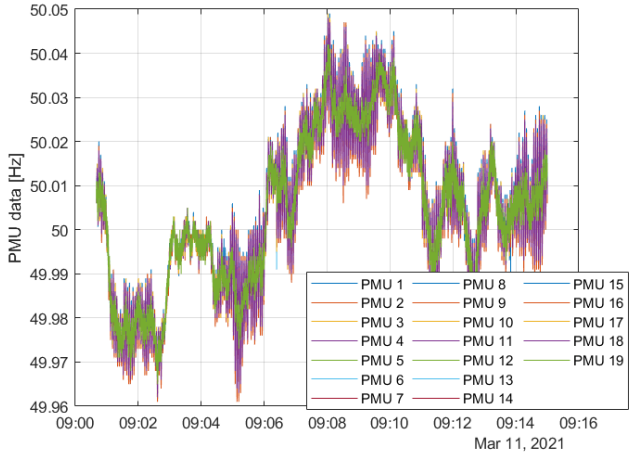

Fig. 13. Frequencies acquired in March 2021.

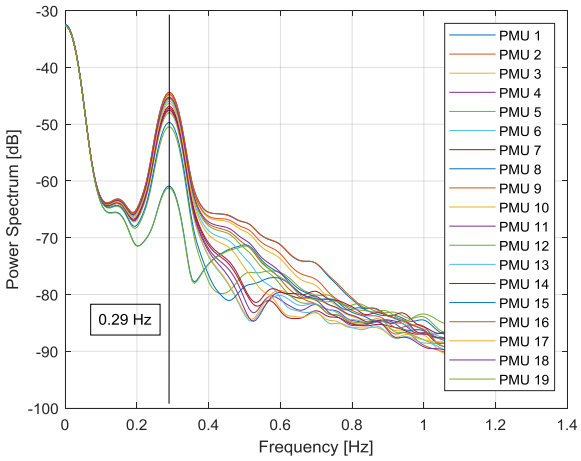

Fig. 14. Power spectrum of time window considered.

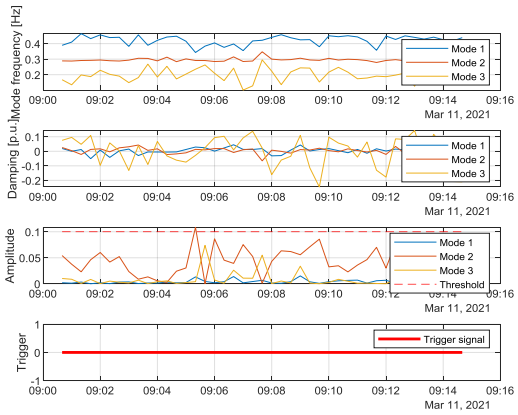

Fig. 15. Frequency, damping, and amplitude identified by the proposed approach along with trigger status.

D. Range of Effectiveness of Proposed Approach

Concerning the assessment of the suitability of using a fixed threshold, Fig. 16 and Fig. 17 present the probability density function of the modal amplitude and frequency estimated in 2021 (S-N mode). The average modal amplitude is well below the threshold of 0.10 p.u., whereas the frequency is centered at approximately 0.30 Hz. These two figures prove the quality of the selected approach and settings against the variability of the operating conditions such as the topology and generation pattern.

Table I lists the average computational time of 20 s sliding window (computed considering data detrending, data packet reconstruction, data filtering, and mode identification) of the events shown in this study and two additional events (events 1 and 2). Computations have been performed on an Intel® Core™ i7-9750H CPU @ 2.60 GHz laptop. The average values are always less than 100 ms, making the proposed approach suitable for real-time monitoring using a reasonable number of inputs.

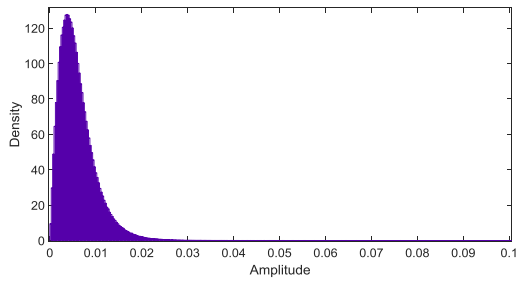

Fig. 16. Probability density function of modal amplitude estimated in 2021.

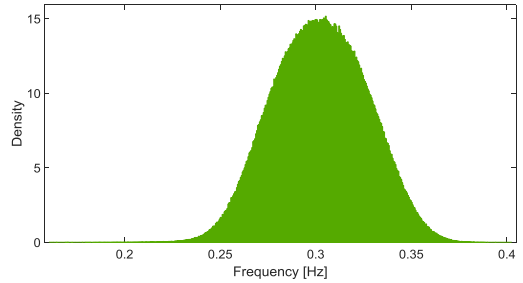

Fig. 17. Probability density function of modal frequency estimated in 2021.

TABLE I
AVERAGE COMPUTATIONAL TIME OF 20 S SLIDING WINDOW

Event	Number of processed PMUs	Length of data analyzed (min)	Average computational time of 20 s window (s)
Oscillatory event of 2017	12	25	0.06
Short-circuit event of 2019	17	17	0.07
Normal grid operation of 2021	19	15	0.07
Event 1	22	10	0.07
Event 2	33	16	0.10

V. CONCLUSION

This study presents the practical implementation of the block-enhanced DMD approach adopted by Terna in its control room for the real-time monitoring of frequency oscillations in the Italian power system and presents the approach along with the criteria set to generate a reliable alarm signal in the case of critical interarea oscillations in a real power system. Such criteria are the outcome of a massive testing campaign conducted in 2020 and 2021. Its adoption in the control room makes it possible to alert operators in the case of sustained interarea oscillations. The approach utilizes the most interesting properties of the DMD approach, such as decomposition over time and space, optimization over a time window, accuracy, robustness, information content, limited computational complexity, and the possibility of exploiting its properties in real-time. Different variants are tested and the best approach is set and tuned. The performance is validated using the presented results and analyses. The adopted indices, threshold set, and overall monitoring system are demonstrated to be very reliable and robust under different operating conditions, e. g., such as low/high load, low/high RES penetration, and network topology changes.

REFERENCE

[1] ENTSO-E. (2017, Jul.). Analysis of CE inter-area oscillation of 1st December 2016. [Online]. Available: https://eepublicdownloads.entsoe.eu
[2] ENTSO-E. (2018, Mar.). Oscillation event 03.12.2017 system protection and dynamics WG. [Online]. Available: https://eepublicdownloads.entsoe.eu
[3] E. M. Carlini, G. M. Giannuzzi, R. Zaottini *et al*., "Parameter identification of interarea oscillations in electrical power systems via an improved hilbert transform method," in *2020 55th International Universities Power Engineering Conference (UPEC)*, Sept. 2020, Turin, Italy.
[4] D. Lauria and C. Pisani, "On Hilbert transform methods for low frequency oscillations detection," *IET Generation, Transmission & Distribution*, vol. 8, no. 6, pp. 1061-1074, Jun. 2014.
[5] D. Lauria and C. Pisani, "Improved non-linear least squares method for estimating the damping levels of electromechanical oscillations," *IET Generation, Transmission & Distribution*, vol. 9, no. 1, pp. 1-11, Jan. 2015.
[6] F. Bonavolonta, L. P. D. Noia, A. Liccardo *et al*., "A PSO-MMA method for the parameters estimation of interarea oscillations in electrical grids," *IEEE Transactions on Instrumentation and Measurement*, vol. 69, no. 11, pp. 8853-8865, Jun. 2020.
[7] R. Vaz, G. R. Moraes, E. H. Z. Arruda *et al*., "Event detection and classification through wavelet-based method in low voltage wide-area monitoring systems," *International Journal of Electrical Power & Energy Systems*, vol. 130, p. 106919, Sept. 2021.
[8] A. Bosisio, A. Berizzi, G. R. Moraes *et al*., "Combined use of PCA and Prony analysis for electromechanical oscillation identification," in *Proceeding of 7th Int. Conf. Clean Electr. Power Renew. Energy Resour. Impact*, Jul. 2019, pp. 62-70, Otranto, Italy.
[9] P. J. Schmid, "Dynamic mode decomposition of numerical and experimental data," *Journal of Fluid Mechanics*, vol. 656, pp. 5-28, Jul. 2010.
[10] J. N. Kutz, S. L. Brunton, B. W. Brunton *et al*., *Dynamic Mode Decomposition*. Siam, Philadelphia, 2016.
[11] E. Barocio, B. C. Pal, N. F. Thornhill *et al*., "A dynamic mode decomposition framework for global power system oscillation analysis," *IEEE Transactions on Power Systems,* vol. 30, no. 6, pp. 2902-2912, Dec. 2015.
[12] S. Mohapatra and T. J. Overbye, "Fast modal identification, monitoring, and visualization for large-scale power systems using dynamic mode decomposition," in *Proceeding of 19th Power Systems Computation Conference,* Aug. 2016, Genoa, Italy.
[13] A. Berizzi, A. Bosisio, R. Simone *et al*., "Real-time identification of electromechanical oscillations through dynamic mode decomposition," *IET Generation Transmission and Distribution*, vol. 14, no. 19, pp. 3992-3999, Jul. 2020.
[14] L. Wang, G. Cai, Z. Chen *et al*., "Dominant inter-area oscillation mode identification using local measurement and modal energy for large-scale power systems with high grid-tied VSCs penetration," *International Journal of Electrical Power & Energy Systems*, vol. 117, p. 105697, May 2020.
[15] I. Scherl, B. Strom, J. K. Shang *et al*., "Robust principal component analysis for modal decomposition of corrupt fluid flows," *Physical Review Fluids*, vol. 5, no. 5, p. 054401, May 2020.
[16] D. Yang, H. Gao, G. Cai *et al*., "Synchronized ambient data-based extraction of interarea modes using Hankel block-enhanced DMD," *International Journal of Electrical Power & Energy Systems,* vol. 128, p. 106687, Jun. 2021.
[17] M. Zuhaib and M. Rihan, "Identification of low-frequency oscillation modes using PMU based data-driven dynamic mode decomposition algorithm," *IEEE Access*, vol. 9, pp. 49434-49447, Mar. 2021.
[18] N. Mohan, K. P. Soman, and S. S. Kumar, "Wide-area monitoring of power system using dynamic mode decomposition on nonlinear observables," in *15th IEEE India Council International Conference (INDICON)*, pp. 1-5, Dec, 2018, Coimbatore, India
[19] A. Alassaf and L. Fan, "Randomized dynamic mode decomposition for oscillation modal analysis," *IEEE Transactions on Power Systems*, vol. 36, no. 2, pp. 1399-1408, Jul. 2021.
[20] S. Zhou, G. Cai, D. Yang *et al*., "Ambient data-driven oscillation

modes extraction using output-only observer/Kalman filter identification and dynamic mode decomposition," in *Proceeding of 2021 IEEE 4th International Electrical and Energy Conference (CIEEC)*, May 2021, Wuhan, China.
[21] A. Saija, K. Sonam, F. Kazi *et al*., "Coherency identification in multi-machine power systems using dynamic mode decomposition," in *Proceeding of European Control Conference (ECC)*, St. Petersburg, Russia, Jul. 2020, pp. 1342-1347.
[22] M. Netto, V. Krishnan, L. Mili *et al*., "Real-time modal analysis of electric power grids-the need for dynamic state estimation," in *International Conference on Probabilistic Methods Applied to Power Systems (PMAPS)*, Liege, Belgium, Sept. 2020.
[23] D. Yang, B. Wang, G. Cai *et al*., "Data-driven estimation of inertia for multiarea interconnected power systems using dynamic mode decomposition," *IEEE Transactions on Industrial Informatics*, vol. 17, no. 4, pp. 2686-2695, Apr. 2021.
[24] C. Olivieri, F. de Paulis, A. Orlandi *et al*., "Estimation of modal parameters for inter-area oscillations analysis by a machine learning approach with offline training," *Energies*, vol. 13, no. 23, p. 6410, Dec. 2020.
[25] S. L. Brunton and J. N. Kutz, *Data-driven Science and Engineering*. Cambridge: Cambridge University Press, 2019.
[26] J. C. A. Barata and M. S. Hussein, "The Moore-Penrose pseudoinverse: a tutorial review of the theory," *Brazilian Journal of Physics*, vol. 42, no. 1-2. pp. 146-165, Apr. 2012.
[27] R. B. Leandro, A. S. e Silva, I. C. Decker *et al*., "Identification of the oscillation modes of a large power system using ambient data," *Journal of Control, Automation and Electrical Systems volume*, vol. 26, no. 4, pp. 441-453, Apr. 2015.
[28] D. J. Trudnowski, J. W. Pierre, N. Zhou *et al*., "Performance of three mode-meter block-processing algorithms for automated dynamic stability assessment," *IEEE Transactions on Power Systems*, vol. 23, no. 2, pp. 680-690, May 2008.
[29] J. Kou and W. Zhang, "An improved criterion to select dominant modes from dynamic mode decomposition," *European Journal of Mechanics - B/Fluids*, vol. 62, pp. 109-129, March–April 2017.
[30] M. R. Jovanović, P. J. Schmid, and J. W. Nichols, "Sparsity-promoting dynamic mode decomposition," *Physics of Fluids*, vol. 26, no. 2, pp. 1-22, Feb. 2014.
[31] P. Kundur, N. J. Balu, and M. G. Lauby, *Power System Stability and Control*. New York: McGraw-Hill, 1994.
[32] M. Brown, M. Biswal, S. Brahma *et al*., "Characterizing and quantifying noise in PMU data," in *Proceeding of 2006 IEEE PES General Meeting*, Boston, USA, Jul. 2016.
[33] C. Zhang, Y. Zhao, L. Zhu *et al*., "Implementation and hardware-in-the-loop testing of a wide-area damping controller based on measurement-driven models," in *Proceeding of 2021 IEEE PE S General Meeting*, Washington DC, USA, Jul. 2021, pp. 1-5.
[34] L. Zhu, W. Yu, Z. Jiang *et al*., "A comprehensive method to mitigate forced oscillations in large interconnected power grids," *IEEE Access*, vol. 9, pp. 22503-22515, Feb. 2021.

Andrea Vicario received the M.Sc. degree in electrical engineering in 2018 from Politecnico di Milano, Milan, Italy. He is currently pursuing the Ph.D. degree in electrical engineering at Politecnico di Milano. He has been Assistant Professor at Politecnico di Milano since 2021. His research interests include power system dynamics, stability, and wide-area monitoring.

Alberto Berizzi received the Ph.D. degree in electrical engineering at Politecnico di Milano, Milan, Italy in 1994. He was an Assistant Professor at the Politecnico di Milano, from 1992 to 1998. Since 2006, he has been a Full Professor of electric power systems. His research is testified by more than 200 papers and publications dealing with power system analysis, security, and optimization. His research interests include power system security, voltage/reactive power management, RES integration in power systems.

Giorgio M. Giannuzzi received the Ph.D. degree in electrical engineering from the University of Rome, Rome, Italy. He has been working at ABB until 2000, in Rome and Milan (Italy), Helsinki (Finland), Ladenburg (Germany) and Raleigh (USA). Since 2001, he has been working at Terna, Rome, as an Expert in dynamic studies, protection, telecontrol, substation automation, wide area defence system and wide area monitoring system. Under his guidance, the Terna EMS (optimal power flow security and market constrained, optimal reactive power flow, dynamic security assessment tool, dynamic and static security verification software, and operator training simulator) was designed. He supervised the Italian Grid Code technical enclosures (primary and secondary frequency regulation, load shedding, protection and automation, and defence plans). He has been a member of the UCTE Expert Group on power system stability and, since 2010, he joined the ENTSO-E System Protection and Dynamics Group. Since 2014, he has been Convenor, coordinating the European evaluation over-dispersed generation impact on system security and load shedding. He is currently responsible for the Engineering Department of National Dispatching Centre. His research interests include defence systems, WAMS, WADC, WAPS, protection systems, modal analysis, simulations and tools (RMS and EMT), dynamics of generators (AVR, Prime Movers, PSS, dynamic models).

Cosimo Pisani received the Ph.D. degree in electrical engineering from the University of Naples Federico II, Naples, Italy, in 2014. During his Ph.D. in collaboration with Terna, he investigated dynamic stability issues of large interconnected power systems, such as the European one. He is currently the Head of Stability and Network Logics at the Dispatching and Switching Department of Terna, Rome, Italy. He is the author or co-author of over 80 scientific articles in the IEEE and CIGRE communities. He is a Leader of the WAMS Task Force within ENTSO-E System Protection and Dynamic and Italian representative of CIGRE Study Committee C4 System Technical Performance. His research interests include applications of dynamic stability of power systems, wide-area monitoring and protection systems, high-voltage direct current systems, and power system restoration.